iScience

Article

Islet single-cell transcriptomic profiling during obesity-induced beta cell expansion in female mice

Graphical abstract

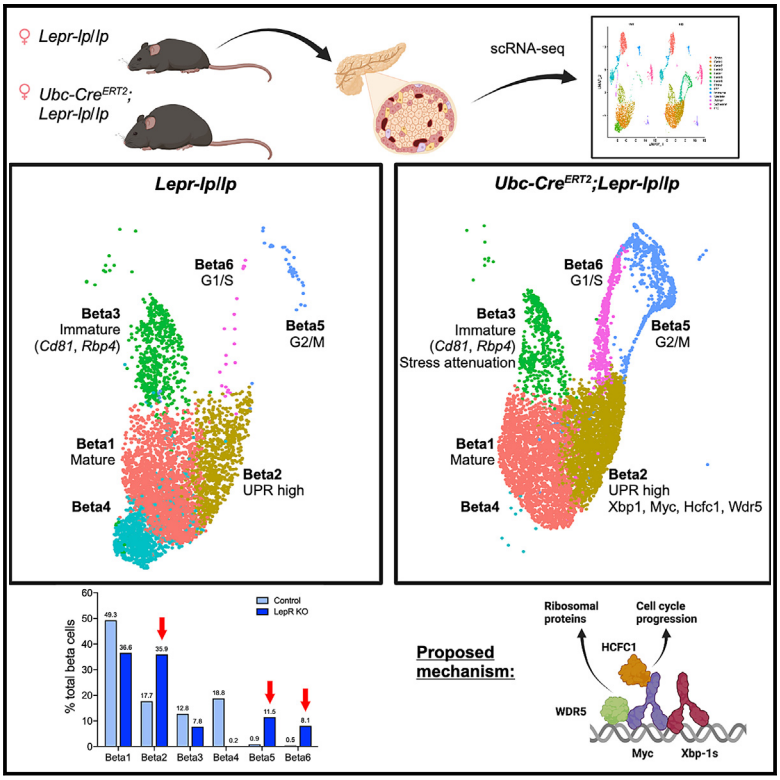

Highlights

- Islet transcriptional responses during early metabolic adaptations to obesity
- Beta cells undergoing UPR upregulate protein translation and cell cycle gene programs
- UPR beta cells enrich for Xbp1 and Myc target genes
- Suggest Xbp1 and Myc coordination alleviate UPR and stimulate beta cell proliferation

Authors

Peter M. Masschelin, Scott A. Ochsner, Sean M. Hartig, Neil J. McKenna, Aaron R. Cox

Correspondence

richard.a.cox@uth.tmc.edu

In brief

Biological sciences; Cell biology; Specialized functions of cells; Functional aspects of cell biology.

Masschelin et al., 2025, iScience *28*, 112031
March 21, 2025
https://doi.org/10.1016/j.isci.2025.112031

CellPress

iScience

CellPress
OPEN ACCESS

Article

Islet single-cell transcriptomic profiling during obesity-induced beta cell expansion in female mice

Peter M. Masschelin,[1,2] Scott A. Ochsner,[2] Sean M. Hartig,[1,2] Neil J. McKenna,[2] and Aaron R. Cox[1,3,4,*]
[1]Division of Diabetes, Endocrinology, and Metabolism, Department of Medicine, Baylor College of Medicine, Houston, TX 77019, USA
[2]Department of Molecular and Cellular Biology, Baylor College of Medicine, Houston, TX, USA
[3]Center for Metabolic and Degenerative Diseases, Institute of Molecular Medicine, Univeristy of Texas Health Science Center at Houston, Houston TX 77019, USA
[4]Lead contact
*Correspondence: richard.a.cox@uth.tmc.edu
https://doi.org/10.1016/j.isci.2025.112031

SUMMARY

Targeting beta cell proliferation is an appealing approach to restore glucose control in type 1 diabetes. However, the underlying mechanisms of beta cell proliferation remain incompletely understood, limiting identification of new therapeutic targets. Obesity is a naturally occurring process that potently induces human and rodent beta cell replication, representing an ideal model to study mechanisms of beta cell proliferation. We showed previously acute whole-body *Lepr* gene deletion in adult mice induces obesity and massive beta cell expansion. Here, using single-cell transcriptomics with female *Lepr* KO islets, we identified distinct populations of beta cells undergoing unfolded protein response (UPR), stress resolution, and cell cycle progression. *Lepr* KO beta cells undergoing UPR markedly increased chaperone protein, ribosomal biogenesis, and cell cycle transcriptional programs that were enriched for Xbp1 and Myc target genes. Our findings suggest a coordinated transcriptional mechanism involving Xbp1 and Myc to alleviate UPR and stimulate beta cell proliferation in obese female mice.

INTRODUCTION

Pancreatic beta cells are lost in type 1 diabetes (T1D) due to autoimmune destruction causing insulin deficiency and high glucose levels. Strategies that regenerate or replace beta cells are a long sought after therapy to potentially cure T1D. Similarly, individuals with type 2 diabetes (T2D) may benefit from a regenerative therapy, as T2D progression is associated with significant beta cell loss due to beta cell stress, exhaustion, and gluco/lipo-toxicity.[1,2] Of note, beta cells undergo compensatory beta cell expansion in obese individuals without diabetes to meet the insulin demand and maintain glucose homeostasis, but the mechanism remains to be determined.

Insulin-producing beta cells are formed during fetal development from pancreas progenitor cells through two waves of differentiation followed by cell replication. In the postnatal pancreas, beta cells expand primarily through self-replication. While rare and heterogeneous populations of cells have been identified in the islet,[3–14] the adult pancreas is largely known to lack a stem/progenitor cell that meaningfully contributes to the beta cell pool.[15–17] The elusiveness of a true adult pancreas or islet progenitor cell has limited progress for regenerative therapies in diabetes. Thus, mechanisms to activate cell cycle re-entry and beta cell replication have been an area of emphasis for beta cell regeneration.

While progress has been made, mechanisms of beta cell proliferation remain incompletely understood and several challenges still exist.[18,19] Normal adult beta cell proliferation rates are quite low.[20,21] Beta cells are also unresponsive to proliferative stimuli with increasing age.[22,23] However, metabolic adaptation to increasing insulin demand associated with obesity robustly increases beta cell mass. Quantification of beta cells in pancreatic sections from persons who were obese demonstrates a significant increase in beta cells.[2,24] Mouse models of obesity similarly demonstrate robust increases in beta cell mass.[25–27] Despite these observations, durable mechanisms that connect metabolism to beta cell proliferation are lacking. Part of the challenge is that congenic mutant mice are not suitable for studying adult beta cell expansion, while dietary interventions generate variable phenotypes.[26] We previously generated a genetically inducible mouse model of obesity through tamoxifen mediated Cre recombination to delete the leptin receptor (*Lepr*).[17] Mice with whole body *Lepr* gene deletion (*Ubc-Cre^{ERT2};Lepr$^{lp/lp}$*) exhibit dramatic weight gain accompanied by massive beta cell proliferation that results in a doubling of beta cell mass within 3 weeks. The advantages of *Lepr* knockout (KO) mice include avoidance of developmental impacts on beta cells associated with constitutive disruption of leptin signaling (*ob/ob*, *db/db* mice), they do not develop frank diabetes (*db/db* mice), and beta cell mass is maintained beyond 7 months of age.[17,28,29] Therefore, acute *Lepr* knockout (KO) mice represent a robust model to study mechanisms of beta cell proliferation. Our goal was to leverage the naturally occurring process of obesity that potently induces human and rodent beta cell replication, to define mechanisms for beta cell regeneration.

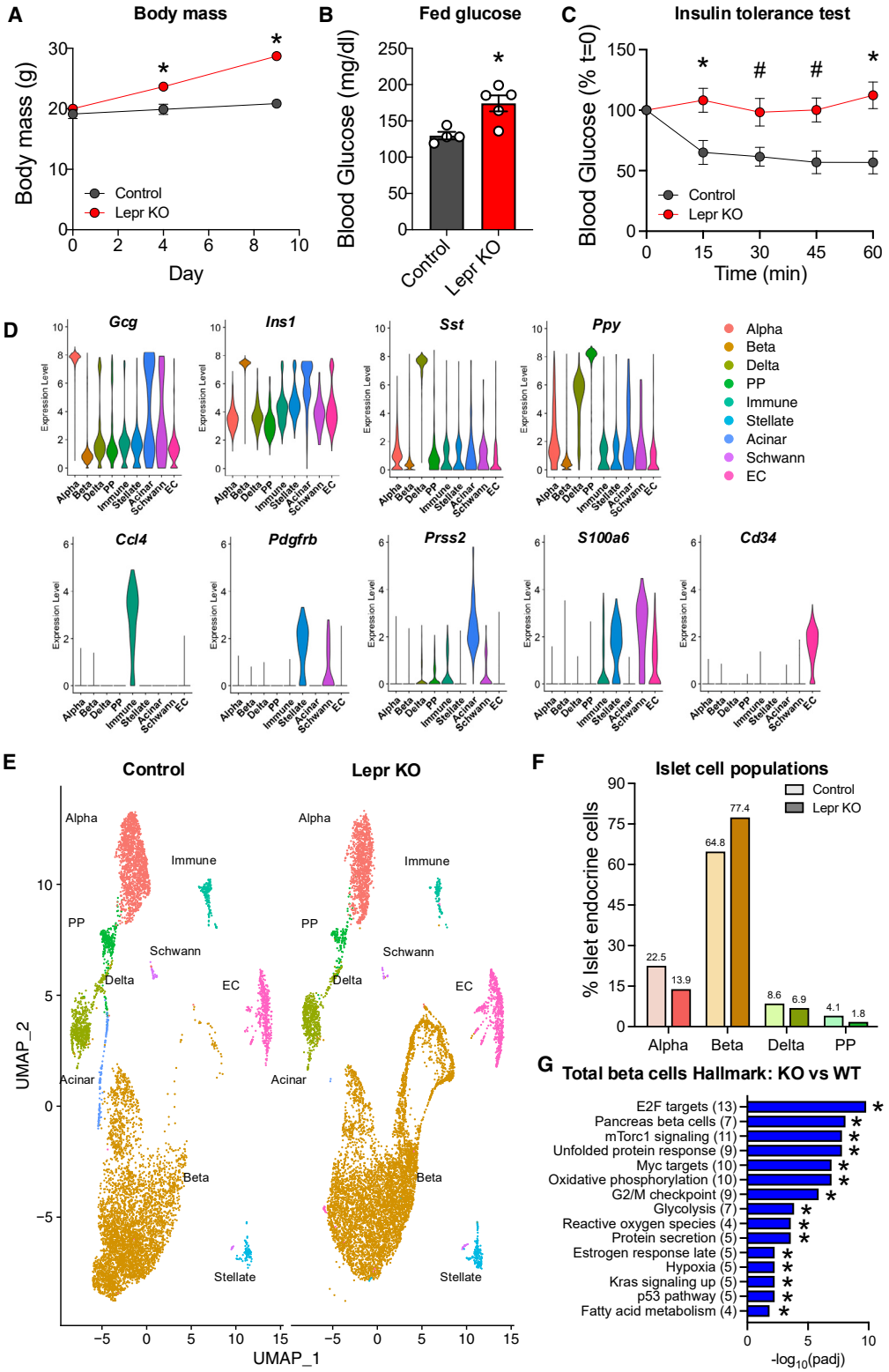

(legend on next page)

Defining the systemic signal that can drive beta cells to replicate has been challenging and potentially derives from multiple factors working together. Several studies demonstrate glucose is a durable stimulus for beta cell proliferation,[30–32] but potentially not the sole factor in obesity. Insulin resistance induced liver derived factors have been postulated to stimulate beta cell proliferation,[33,34] as well as neural signals,[35] bone-related signaling pathways,[36] and myokines[37] have also been implicated as possible beta cell mitogens; although in some cases a paucity of follow-up studies suggest some limitations in translating these efforts. Considering the complexity of systemic physiologic changes and organs affected in obesity, we focused on changes intrinsic to the beta cell that may be more easily defined and targeted therapeutically. To this end, we used single-cell transcriptomics to identify gene networks and signaling pathways central to beta cell proliferation that may reveal targets to expand beta cells for treating diabetes.

RESULTS

Single cell transcriptome analysis of islets following acute whole body *Lepr* KO in female mice

Obesity is a powerful stimulus to increase beta cell proliferation, but the underlying mechanisms are not well defined. We previously showed acute whole body *Lepr* KO doubles beta cell mass within 3 weeks and represents an excellent model to capture the mechanisms regulating obesity-induced beta cell proliferation. Here, we treated 3-month-old female *Ubc-Cre^{ERT2};Lepr$^{lp/lp}$* (*Lepr* KO) and *Lepr$^{lp/lp}$* littermate controls with tamoxifen to induce *Lepr* deletion in Cre positive mice, as previously.[17] On average control mice gained 1.7 g in body mass over 9 days, while the *Lepr* KO mice gained 8.7 g (Figure 1A), consistent with a loss of LEPR function causing hyperphagia, and leading to hyperglycemia and insulin resistance (Figures 1B and 1C). We isolated islets on day 9, which occurs during a period (day 7–13) when over 50% of beta cells proliferate,[17] and pooled islets (4 mice/group) for scRNA-seq. Uniform manifold approximation and projection (UMAP) revealed 16 cell clusters (Figure S1) that we identified using known marker genes (Figure 1D) and subsequently confirmed by differential gene expression analysis (Table S1). Interestingly, six beta cell populations and three endothelial cell populations were observed (Figure S1) that were each grouped together for initial analyses (Figures 1D–1G). In total, we identified four primary islet endocrine cell types, alpha (*Gcg*), beta (*Ins2*), delta (*Sst*), and PP (*Ppy*) cells and non-endocrine cell types including immune (*Ccl4*), stellate (*Pdgfrb*), acinar (*Prss2*), Schwann (*S100a6*), and endothelial cell clusters (*Cd34*; EC) (Figures 1D and 1E, Figure S1, Table S1). Within the islet endocrine cells, we found the total beta cells represented a greater percentage within the *Lepr* KO samples (77.4%) compared to control (64.8%) (Figures 1E and 1F, Table S2). These data are consistent with our previous histologic analysis demonstrating beta cell expansion following *Lepr* KO.[17] Gene set enrichment analysis of significantly upregulated genes in total beta cells (Table S3) of *Lepr* KO islets revealed several pathways involved in metabolism (oxidative phosphorylation, glycolysis, fatty acid metabolism), cell proliferation (E2F targets, mTorc1 targets, Myc targets, G2/M checkpoint), and the unfolded protein response (UPR) (Figure 1G, Table S4). Collectively, our results indicated that obesity induces metabolism and cell cycle gene programs associated with beta cell expansion in *Lepr* KO mice.

Acute *Lepr* KO induces shift in beta cell subpopulation abundance

To identify genes that define each individual beta cell cluster, we subsetted the six beta cell clusters from all other cells for further analysis (Figure 2A). There was an obvious shift in cell abundance for each cluster between control and *Lepr* KO samples (Figure 2B, Table S2). We detected more cells in the Beta2, Beta5, and Beta6 clusters within *Lepr* KO islets, fewer cells in the Beta1 and Beta3 clusters, and a near absence of cells in Beta4 compared to control. We next looked at expression of known beta cell transcription factors and functional markers (Figure 2C). In general, expression was similar across clusters, except for the Beta3 cluster that tended to have higher expression of *Chga* and *Chgb*, but lower expression of *Ins1*, *Ins2*, *Mafa*, and *Ucn3*, suggesting the Beta3 cluster represents immature cells. Consistent with this, differential gene expression applied to the six clusters revealed Beta3 cells expressed non-beta endocrine markers, including *Sst*, *Pyy*, *Ppy*, *Gcg*, and *Rbp4* (Figure 2D, Table S5). The top differentially expressed genes (DEG) in Beta4 encoded digestive enzymes primarily associated with acinar cells (*Cela2a*, *Clps*, *Ctrb1*, *Pnlip*, *Cela3b*, *Prss2*, *Try4*, *Camk2n1*, *Sycn*) (Figure 2D, Table S5). While Beta3 and Beta4 clusters differentially expressed non-beta cell marker genes relative to the other beta cell clusters (Figure 2D, Table S5), the magnitude of expression was lower than found in cognate cells (i.e., *Gcg* - alpha cells, *Prss2* – acinar cells) (Figures 1D and 2E). Accordingly, Beta3 cells differentially expressed *Cd81* and *Rbp4* (Figure 2F) that are known markers of immature beta cells with reduced exocytotic activity.[11,13,38] Only four genes defined the Beta1 cluster (*Mt1*, *Nupr1*, *Mt2*, *Ftl1*) (Figure 2D, Table S5). Among the top DEG in the Beta2 cluster were several chaperone and stress response proteins (*Fkbp11*, *Sdf2l1*, *Hspa5*, *Ssr4*, *Dnajc3*, *Pdia6*, *Hsp90b1*,

Figure 1. Single cell transcriptome analysis following acute whole body *Lepr* KO

(A) Body mass (g) from the start of tamoxifen treatment (day 0) until islet harvest (day 9) (n = 4/group). Mean ± SEM; *$p < 0.05$ by two-way ANOVA.

(B) Fed glucose levels (mg/dL) and C) insulin tolerance test (% initial glucose at time = 0 min) (n = 4–6/group). Mean ± SEM; *$p < 0.05$, #$p < 0.09$ by (b) t-test or (C) two-way ANOVA.

(D) Cell type specific marker gene expression for alpha (glucagon; *Gcg*), beta (insulin 1; *Ins1*), delta (somatostatin; *Sst*), Ppy (pancreatic polypeptide; *Ppy*), immune (*Ccl4*), stellate (*Pdgfrb*), acinar (*Prss2*), Schwann (*S100a6*), and endothelial (*Cd34*).

(E) UMAP plot of single cell RNA-seq from control (left; *Lepr-lp/lp*) and *Lepr* KO (right; *Ubc-Cre;Lepr-lp/lp*) islets. Also see Figure S1.

(F) Relative abundance of hormone producing cells as a percentage of total islet endocrine cells within control and *Lepr* KO islets analyzed from scRNA-seq.

(G) Hallmark enrichment analysis of genes significantly upregulated in total beta cells from *Lepr* KO islets compared to control (*$p < 0.05$ by hypergeometric test for overrepresentation).

(D–G) The total cells analyzed included 7975 cells from control islets and 9406 cells from *Lepr* KO islets.

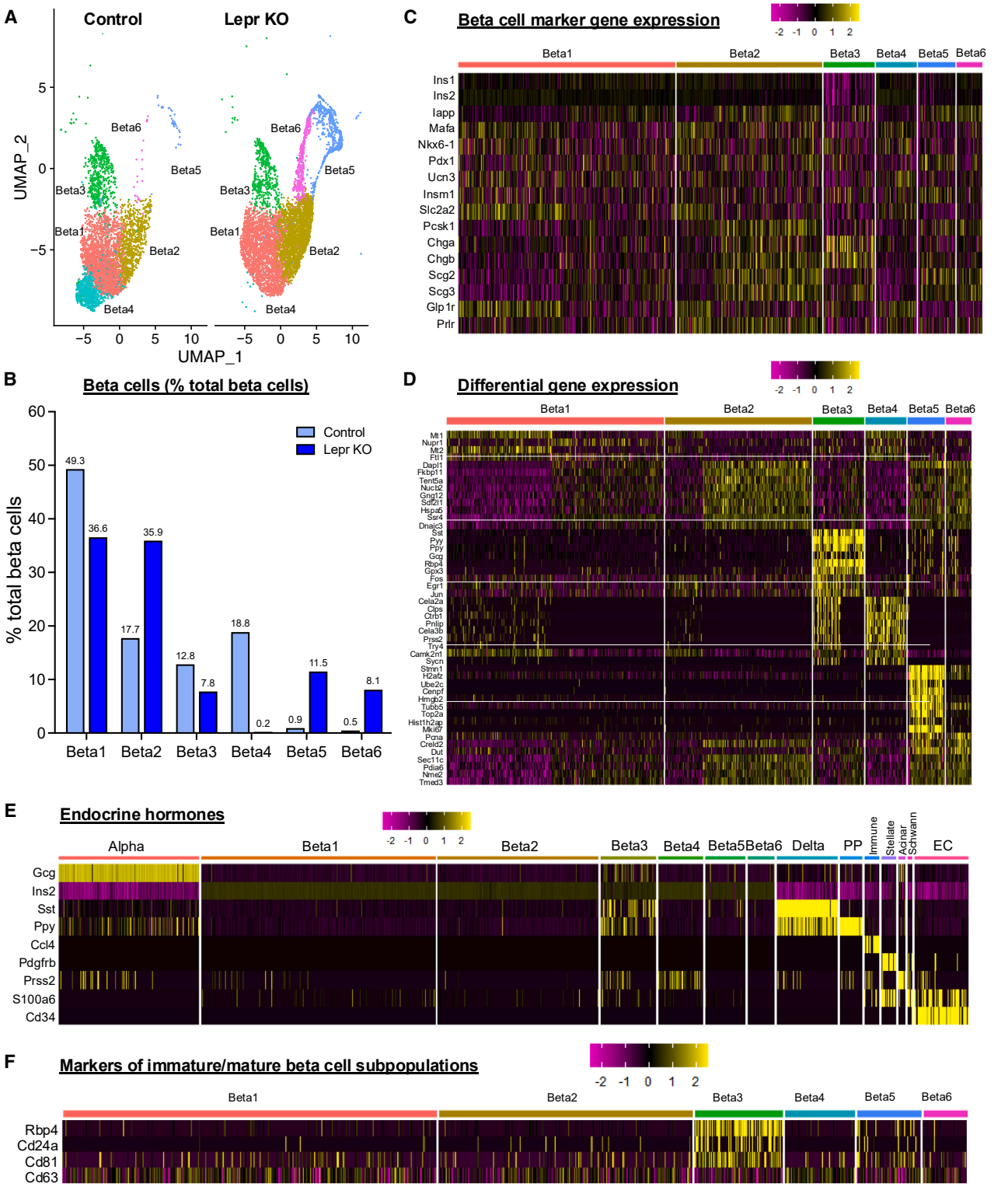

Figure 2. Acute *Lepr* KO induces shift in beta cell subpopulation abundance

(A) Six beta cell subpopulations were identified by differential gene expression analysis as shown by the UMAP plot.

(B) Relative abundance of beta cell subpopulations as a percentage of total beta cells from control and *Lepr* KO islets (percentages shown above the bar).

(C) Heatmap of beta cell marker gene expression across beta cell subpopulations.

(legend continued on next page)

Calr, *Srpr*, *Dnajb9*, *Hyou1*) (Figure 2D; Table S5), suggestive of beta cells undergoing ER stress and the UPR commonly observed in beta cell scRNA-seq datasets.[9,39–41] Lastly, cell cycle genes defined the Beta5 and Beta6 clusters (Figure 2D, Table S5), which contained very few cells in control (1.4%) but accounted for 19.6% of all beta cells in *Lepr* KO islets (Figure 2B, Table S2). Collectively, *Lepr* KO beta cells exhibited an increased proportion of cells expressing UPR (Beta2) and cell cycle marker genes (Beta5, Beta6), consistent with increased beta cell proliferation in obese mice.[17]

Acute *Lepr* KO induces cell cycle entry and progression

Beta cells are typically quiescent, but can be stimulated to re-enter the cell cycle. Our differential gene expression analysis indicated two beta cell clusters, particularly in *Lepr* KO islets (Figure 2B), are defined by cell cycle genes (Figure 2D). To further define these clusters, we performed Cell Cycle Scoring to look at gene expression by cell cycle phase. While the majority of cells were found to be in G1 phase, the Beta6 cluster cells map to S phase and Beta5 cells map to G2/M phase (Figure 3A). Accordingly, Beta5 cells highly expressed genes (*Ccna2*, *Ccnb1*, *Ccnb2*, and *Cdk1*) enriching for Reactome pathways ''Mitotic spindle checkpoint'', ''Separation of sister chromatids'', and ''M phase'' (Figures 3B and 3C; Table S5). In contrast, Beta6 cells expressed *Pcna*, *E2f1*, *Mcm2*, *Mcm5*, and *Mcm6* that enriched for ''DNA replication'', ''G1/S transition'', and ''S phase'', as well as UPR (Figures 3B and 3C; Table S5). These data demonstrate our studies uniquely capture a very significant proportion (Figure 2B) of beta cells that are progressing through the cell cycle following *Lepr* KO that allows for further interrogation of the gene programs activating cell proliferation.

Acute *Lepr* KO induces an Xbp1 regulated transcriptional program to resolve UPR stress during adaptive beta cell proliferation

We next aimed to define the gene programs activated in the remaining beta cell clusters. DEG in the beta cell clusters (Figure 2D, Table S5) were analyzed by Reactome pathway analysis. The Beta2 cluster genes enriched for ''Unfolded protein response'', ''ATF6 activates chaperones'', and ''IRE1alpha activates chaperones'' pathways (Figure 4A), consistent with the predominant expression of chaperone and UPR genes (*Hspa5*, *Hsp90b1*, *Hyou1*, *Calr*, *Pdia6*, *Dnajc3*, *Srpr*, *Dnajb9*) in the Beta2 cluster (Figure 2D, Table S5). Independently we measured expression of UPR and beta cell genes by qPCR from bulk islet RNA to confirm our observations for *Lepr* KO DEG in total beta cells. *Lepr* KO islets exhibited significantly higher expression of genes encoding chaperone proteins *Hspa5* (*Bip*/*Grp78*) and *Hsp90b1* (*Grp94*) (Figure 4B), without impacting *Xbp1* or *Ddit3* (*Chop*), consistent with the scRNA-seq findings (Table S3). These data suggest *Lepr* KO beta cells undergo adaptive stress response without decompensation.[42] Insulin (*Ins2*) expression was significantly increased in *Lepr* KO islets, consistent with the hyperinsulinemia and beta cell mass expansion observed previously,[17] and *Glut2* (*Slc2a2*) was downregulated by qPCR and scRNA-seq (Figure 4B; Table S3). While Beta2 cells have activated ER stress and UPR responses, the Beta3 cluster cells upregulated genes involved in stress resolution indicated by enrichment for ''Attenuation Phase'' and ''Regulation of HSF1-mediated heat shock response'' (Figure 4A). Beta3 cells differentially increase expression of *Dnajb1*, *Hspa1a*, *Hspa1b*, and *Hspa8* (Table S5) that encode for Hsp40 and Hsp70, the primary inhibitors of Heat shock factor 1 (Hsf1)[43] in the resolution of stress responses. Of note, we observed an overabundance of genes encoding ribosomal proteins expressed in the Beta3 (66 genes) and Beta5 (46 genes) cells (Table S5), which may indicate a positive response to upregulate translation and resolve UPR stress originating in the Beta2 state. Beta4 cells showed enrichment for ''rRNA processing in the mitochondria'' and ''Activation of matrix metalloproteinases''. Lastly, only 4 genes were differentially expressed in Beta1 cells (Figure 2D; Table S5) and were therefore omitted from GSEA, but based on marker gene expression profile (Figure 2C), Beta1 cells represent mature beta cells. Overall, GSEA identification of beta cell clusters is consistent with previous studies,[9,13,40,41] while also revealing for the first time important pathways related to stress resolution in Beta3 cells.

In addition to defining the beta cell subpopulations, we examined DEG between control and *Lepr KO* within each subpopulation (Figure S2; Table S6). *Lepr KO* significantly induced many similar genes and pathways across the beta cell subpopulations, an effect also observed in islets exposed to high-fat diet (HFD) feeding,[13] with protein export and oxidative phosphorylation the predominant enriched pathways (Figure S2; Table S6).[13] Of note, *Lepr KO* significantly increased gene expression of nuclear encoded oxidative phosphorylation in Beta1 cells and chaperone proteins in Beta2 cells (Figure S2; Table S6).

UPR stress resolution involves activation of RNA polymerase II initiation complex and cell cycle regulation in *Lepr* KO beta cells

We previously developed ChIP-seq consensomes,[44–46] which rank genes based on measures of promoter occupancy across publicly available ChIP-seq experiments mapped to a specific immunoprecipitated antigen or signaling node. These consensomes can be used to identify nodes that have high confidence transcriptional target (HCT) intersections (i.e., transcriptional footprints) within gene lists of interest[45,47] – in this case, genes differentially expressed between *Lepr* KO and control for each beta cell cluster (Table S6). To gain insight into regulatory networks contributing to cell fate decisions between beta clusters,

(D) Heatmap of differentially expressed genes for each beta cell subpopulation.
(E) Heatmap of islet hormone expression across beta cell clusters, alpha, delta, and PP cells, as well as immune, stellate, acinar, Schwann, and endothelial (EC) cells.
(F) Heatmap of immature and mature marker gene expression across beta cell subpopulations.
The total beta cells analyzed included 4567 beta cells from control islets and 6545 beta cells from *Lepr* KO islets. Alpha cells from control = 1586 and *Lepr* KO = 1174 cells, for delta cells from control = 606 and *Lepr* KO = 585 cells, and for PP from control = 289 and *Lepr* KO = 148 cells were analyzed.

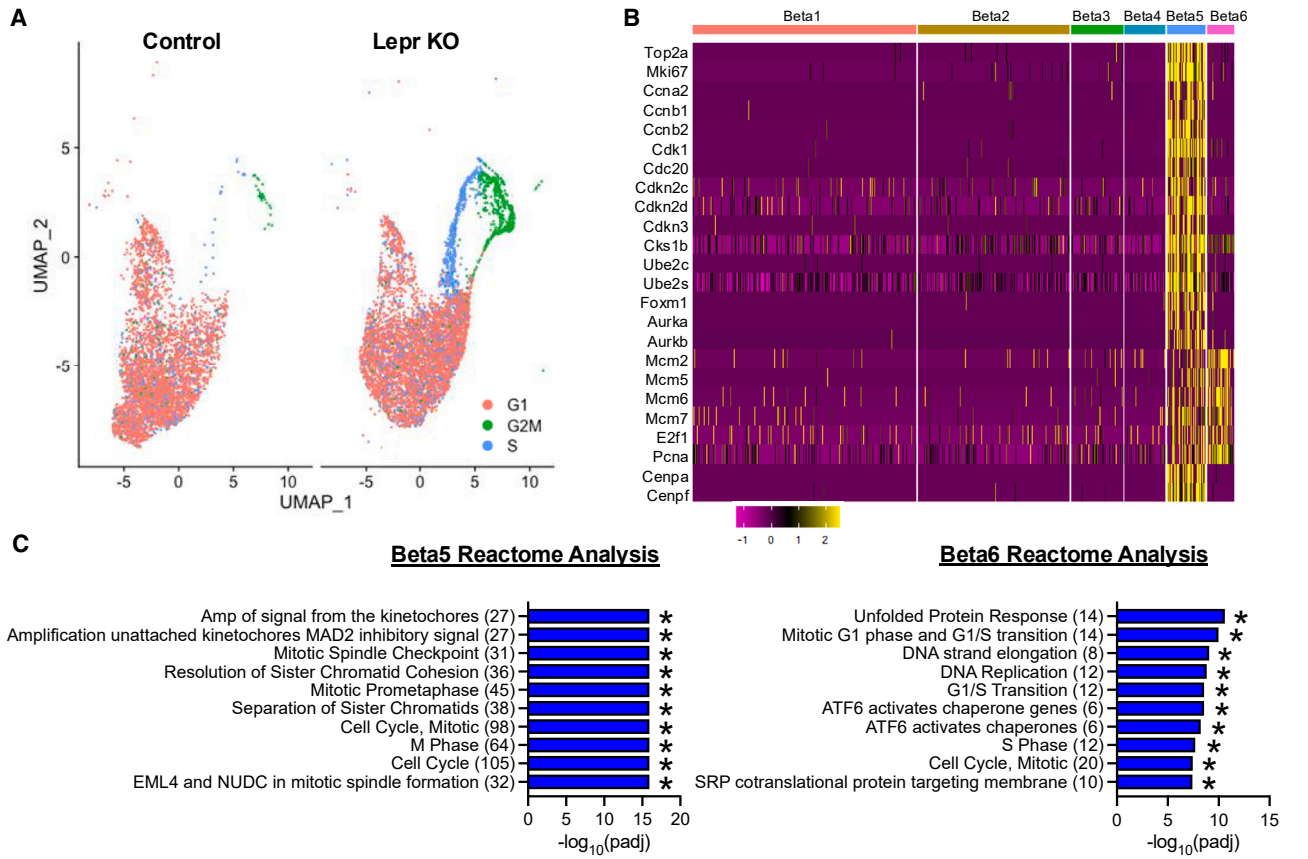

Figure 3. Acute *Lepr* KO activates gene programs associated with cell cycle progression

(A) UMAP plot of beta cells analyzed for enrichment of transcripts in the different cell cycle stages (G1 – pink; S – blue; G2/M – green).

(B) Heatmap of gene expression for markers of S and G2/M phases of the cell cycle across beta cell subpopulations.

(C) Reactome pathway analysis of differentially upregulated genes between control and *Lepr* KO islets for Beta5 (top) and Beta6 (bottom) beta cell subpopulations (*$p < 0.05$ by hypergeometric test for overrepresentation).

The total beta cells analyzed included 4567 beta cells from control islets and 6545 beta cells from *Lepr* KO islets.

we performed HCT intersection analysis to compare induced and repressed transcriptional regulatory networks across the six clusters. Amongst *Lepr* KO upregulated genes in Beta2 cells, the node with the strongest regulatory footprint was XBP1, along with other UPR responsive transcription factors such as HOPX and CREB3L2 (Figure 4C; Table S7). The prominent cell cycle regulator MYC, and its transcriptional co-regulators WDR5 and HCFC1, also exhibited highly significant transcriptional footprints among induced genes in Beta2 cells (Figure 4C; Table S7).

We hypothesized that Beta2 cells undergoing UPR may transition to the Beta3 cluster upon attenuation of stress. HCT intersection analysis resolved a strong identity (p = 3E-04) between the Beta3 KO-downregulated regulatory network and the Beta2 upregulated regulatory network – common nodes included GTF2E2, GTF2B, NELFA, NELFE, TET3, BRD4, SUPT5, HOPX, NELFB, SUPT6, MED12, PHF2, ARID4B, and TBP, among others (Figure 4C, Table S7). This set of nodes enriched for pathways including RNA polymerase II pre-transcription events and HIV Life Cycle (Table S8). Consistent with the attenuation of stress responses (Figure 4A) we further found that one of the strongest nodes with regulatory footprints among Beta3 *Lepr* KO-downregulated genes was that of HSF1 (Table S7). Interestingly, another strong node observed in HCFC1 that coordinately regulates expression of cell cycle genes along with several other enriched nodes (GABPA, ZNF143, YY1; Table S7)[48,49] had significant footprints in *Lepr* KO-induced genes in Beta2 cells (Table S7).

Lepr KO beta cell proliferation involves downregulation of differentiation transcriptional programs

The two beta cell populations demonstrating the largest change in abundance in *Lepr* KO islets were Beta4 (significantly reduced) and Beta5 (significantly increased) cells (Figure 2B; Table S2). To understand potential transcriptional mechanisms underlying the shifts in these populations, we compared regulatory networks for the Beta4 *Lepr* KO upregulated- and Beta5 *Lepr* KO-downregulated gene sets. Common to both gene sets were significant intersection for GTF2B, NELFA, BRD4, NELFB, SUPT5, NELFE, ZMIZ1, TBP, STAT3, TET3, CREBBP, SMAD3, SNAI1, CDK9, SOX4, SMAD4, among others (Figure 4D, Table S7). The intersecting nodes for Beta5 down with Beta4 up (p = 2E-09) were enriched for "Epithelial-Mesenchymal Transition (EMT) during

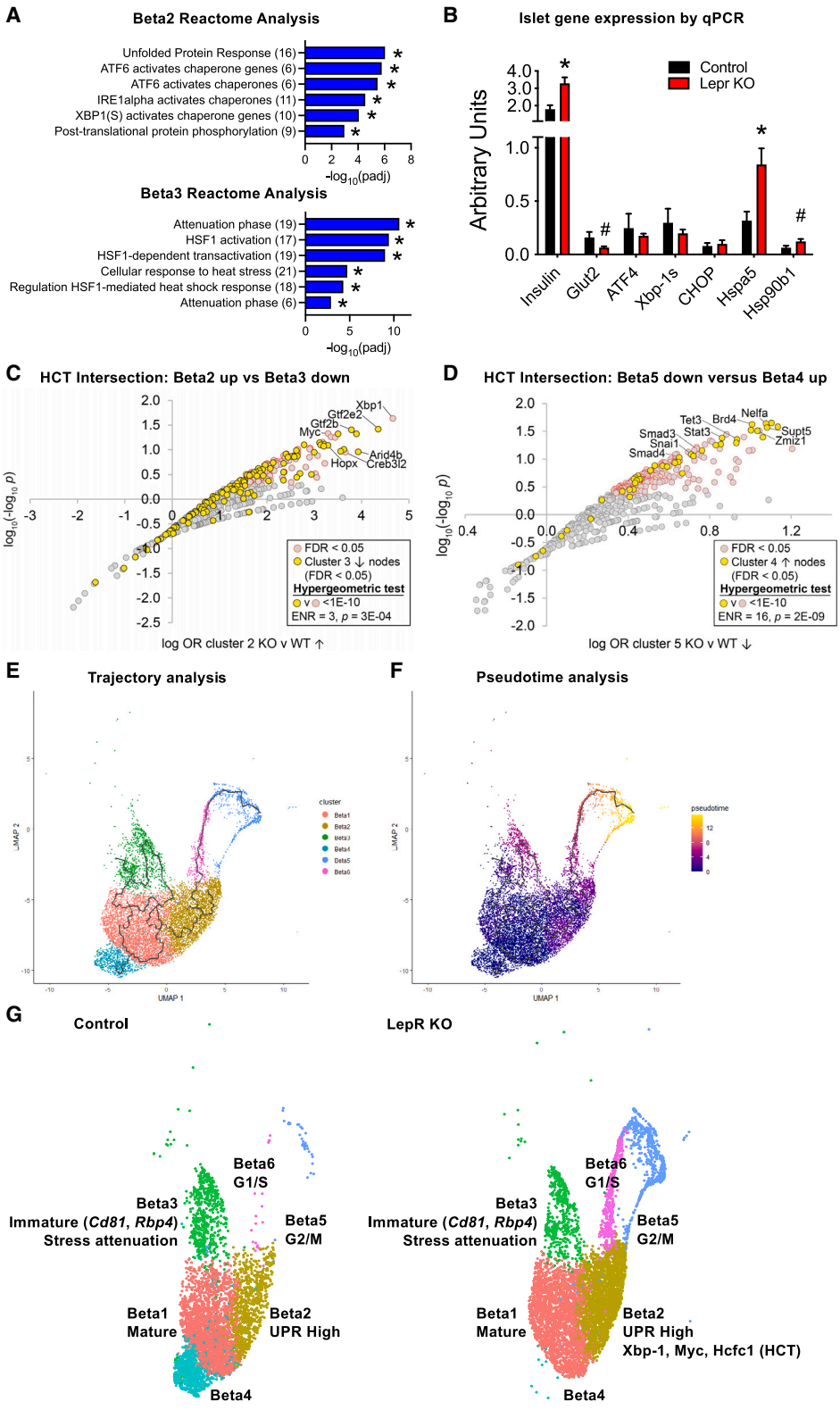

Figure 4. *Lepr* KO induced ER stress response associates with Xbp-1 and Myc activity leading to cell cycle progression

(A) Reactome pathway analysis of differentially expressed genes for Beta2 (top) and Beta3 (bottom) beta cell subpopulations (*$p < 0.05$ by hypergeometric test for overrepresentation).

(legend continued on next page)

gastrulation'', ''Regulation of gene expression in endocrine-committed (NEUROG3+) progenitor cells'', and ''Regulation of beta-cell development'' Reactome pathways (Table S9), which may suggest Beta4 cells have activated beta cell differentiation programs, in contrast to the Beta5 cells that are undergoing cell division (Figures 3A and 3B).

We observed key changes in gene expression and transcriptional regulatory profiles that suggest changes in cell state (differentiation versus proliferation, stress activation versus resolved) following acute *Lepr* KO. To potentially identify transitions between beta cell clusters, we next aligned the transcripts of each individual cell in pseudotime and trajectory analyses. These analyses suggested that beta cells progress from a mature state (Beta1, Beta4) toward one of two states, either a proliferative (Beta5, Beta6) or immature (Beta3) state (Figures 4E and 4F). One notable trajectory branches from Beta1 to Beta2 cells, suggesting a key fate decision that directs beta cells into UPR stress response (Beta2) and then cell cycle re-entry (Beta6, Beta5) (Figures 4E and 4F). Alternatively, trajectories that branch from Beta1 to Beta3 cells form a loop that may suggest a cyclical state change between mature and immature cells (Figures 4E and 4F). Interestingly, the change in beta cell abundance following *Lepr* KO (Figure 2B) suggests beta cells preferentially transition to the UPR-cell cycle trajectory (Beta2, Beta5, and Beta6) and away from an immature state (Beta3) (Figures 4E and 4F). Overall, our findings identify coordinated transcriptional signatures for beta cell subpopulations progressing through stress responses to enter the cell cycle and replicate in response to obesity-associated metabolic demand for greater insulin-producing capacity (Figure 4G).

DISCUSSION

Our objective was to define the transcriptional landscape of pancreatic beta cells during obesity-induced beta cell proliferation. Obesity is a powerful stimulus for beta cell proliferation in rodents[17,25,27] as well as humans,[2,24] and, thus, represents an excellent model to define mechanisms driving beta cell expansion. Single-cell transcriptomic analysis of islets from acute *Lepr* KO mice revealed six beta cell populations, including two substantial populations of proliferating cells (Beta5, Beta6), immature beta cells (Beta3), two mature beta cell populations (Beta1, Beta4), as well as beta cells undergoing UPR (Beta2). Applying a cutting-edge bioinformatics approach that identifies regulatory transcriptional footprints in our dataset, we found that the resolution of UPR stress in *Lepr* KO beta cells involved the attenuation of HSF1 gene regulation and increased ribosomal protein expression associated with prominent XBP1, MYC, and HCFC1 transcriptional activity. These factors potentially coordinate the transition to an immature state (Beta3) or toward UPR stress response (Beta2) leading to re-entry of the cell cycle (Beta5, Beta6) through enhanced expression of chaperone proteins, positive cell cycle regulators, and translation. Overall, our data identifies transcriptional nodes and gene expression profiles of proliferating beta cells in a robust model of beta cell expansion, which provides candidates for targeting regenerative beta cell approaches in diabetes.

Beta cells are mostly post-mitotic with very low proliferation rates in adults[20,21] and, therefore, generally difficult to study transcriptionally. However, the ability to capture beta cells re-entering the cell cycle through single-cell analyses has sparked several studies investigating the transcriptional mechanisms governing beta cell proliferation. Examination of early postnatal mouse beta cells ordered by pseudotime across several timepoints identified proliferative beta cells to be more immature, exhibiting higher expression of regulators of amino acid metabolism and a network of nutrient-responsive transcription factors (SRF, JUNB, FOS, EGR1) with increased reactive oxygen species (ROS) production.[10] Similarly, in pregnancy, *Junb*, *Fos*, and *Egr1* are elevated in islets during compensatory beta cell expansion.[50] In adult rodents, nutrient responses were also found to activate beta cell proliferation associated with ROS. Acute delivery of free fatty acids to rat islets stimulated beta cell proliferation that required MYC transcriptional activity in association with redox responses.[41] Interestingly, mouse beta cells fail to proliferate in the absence of *Myc* during one week of HFD-feeding.[51] Notably, *Myc* expression was highest in a subpopulation of beta cells that enriched for UPR and translation genes.[41] We similarly observed increased MYC transcriptional activity in beta cells with activated UPR following nutrient overload by acute *Lepr* KO, suggesting a tightly coordinated response between Myc and the UPR to increase insulin secretory capacity through beta cell expansion and increased translation. In contrast, beta cell clusters after longer-term HFD studies did not express UPR or cell cycle genes, while *Myc* upregulation was associated with a higher functioning beta cell subset.[13]

Beta cells generally exhibit high levels of ER stress and UPR relative to other cell types,[52] but previous studies identified

(B) Gene expression (fold change) from control (black; *Lepr-lp/lp*) and *Lepr* KO (red; *Ubc-Cre;Lepr-lp/lp*) using total islet RNA (n = 4/group). Mean ± SEM; *$p < 0.05$, #$p < 0.10$ by t-test.

(C) Pathway nodes from the high confidence transcriptional target (HCT) intersection analysis of the Beta2 up gene set (*Lepr* KO vs. control) were plotted as log odds ratio (log OR) against log10(-log10 P) (double-log procedure was used due to the large p-value range). Nodes with significant ($q < 0.05$) HCT intersections with the Beta2 up gene set are colored gray with a red border. Nodes with non-significant ($q > 0.05$) intersections with the Beta2 up gene set are colored gray. A hypergeometric test was performed on the overrepresentation in the $q < 0.05$ nodes of nodes encoded by genes in the Beta3 down gene set, shown in yellow.

(D) Pathway nodes from the HCT intersection analysis of the Beta5 down gene set (*Lepr* KO vs. control) were plotted as log odds ratio (log OR) against log10(-log10 P) (double-log procedure was used due to the large p-value range). Nodes with significant ($q < 0.05$) HCT intersections with the Beta5 down gene set are colored gray with a red border. Nodes with non-significant ($q > 0.05$) intersections with the Beta5 down gene set are colored gray. A hypergeometric test was performed on the overrepresentation in the $q < 0.05$ nodes of nodes encoded by genes in the Beta4 up gene set, shown in yellow.

(E) Trajectory analysis colored by beta cell subpopulation of combined control and *Lepr* KO datasets.

(F) Pseudotime analysis of beta cells of combined control and *Lepr* KO datasets.

(G) Summary of beta cell subpopulations and corresponding state (mature, immature, proliferative) with an overlay of enriched pathways and transcriptional nodes.

(C–G)The total beta cells analyzed included 4567 beta cells from control islets and 6545 beta cells from *Lepr* KO islets.

subpopulations of beta cells indicative of a transition between states of high and low UPR[9,42] that may involve cell cycle re-entry and beta cell proliferation.[9,42,53,54] Alonso and colleagues found beta cell proliferation was more frequent in cells expressing the chaperone protein HSPA5.[42] Accordingly, in *Lepr* KO islets we observed an increased abundance of beta cells undergoing UPR (Beta2) and progressing through the cell cycle (Beta5, Beta6), all of which expressed increased levels of *Hspa5* and other chaperone proteins. XBP1, which positively regulates chaperone protein gene expression, and MYC were identified as the top consensomes amongst upregulated Beta2 genes in *Lepr* KO islets. Interestingly, a link between Xbp1 and Myc has been established in cancer cell lines and patient xenografts. Inhibition of Xbp1 blocked Myc-induced cell proliferation.[55,56] Moreover, XBP1 directly binds MYC to regulate target gene expression.[55] Thus, under conditions of increased demand for insulin production, the UPR and XBP1 may coordinately activate MYC to enhance beta cell proliferation.

Besides promoting cell cycle activator expression,[57] the proliferative effects of Myc are closely connected with its function to stimulate ribosomal biogenesis and translation.[58] Ribosomal biogenesis and protein translation are essential processes that permit cell proliferation.[59] Interestingly, disruption of the UPR sensor IRE1, which activates XBP1, resulted in loss of MYC target gene expression, including downregulation of genes associated with ribosomal and protein export pathways.[56] MYC also interacts with the chromatin-associated protein WDR5 and transcriptional co-regulator HCFC1 to facilitate MYC recruitment to ribosomal protein gene promoters.[60–62] Other studies show HCFC1 is recruited to cell cycle gene promoters at E2F1 binding sites, a key transcription factor regulating G1/S phase progression, and that loss of HCFC1 impairs cell proliferation.[49,63] Together, we observed enrichment of MYC and its co-regulators in a population of beta cells undergoing UPR that enrich for cell cycle and ribosomal genes, as well as XBP1 targeted chaperone protein genes.

In addition to increased cell proliferation, beta cells manage insulin demand through compensatory changes in insulin secretion. Beta cell subpopulations differing by insulin secretory capacity, electrophysiology, and transcriptomics have been described by several groups.[9,11–13,41] Higher functioning beta cell states express identity genes (i.e., *Pdx1*, *Mafa*, *Ins*)[9,11] and surface markers such as *Cd63* and *Cd24*,[12,13] coupled with increased electrical activity and exocytosis. In contrast, lower beta cell function was associated with decreased expression of identity genes, enrichment of non-beta cell genes (*Sst*, *Gcg*, *Ppy*)[12] and elevated expression of *Rbp4* and *Cd81*.[11–13] We similarly identified a population of immature cells that enriched for *Sst*, *Gcg*, *Ppy*, *Rbp4*, *Cd81*, and *Cd24*, with lower expression of beta cell identity genes. It is noteworthy that Beta3 cells expressed *Cd24*, a high functioning marker, while other studies observed no differential expression of the immature maker *Cd81*,[12] reaffirming that multiple markers (and modalities) are necessary to identify beta cell subpopulations. Interestingly, our trajectory analysis revealed a branch that formed a loop between the immature (Beta3) and mature (Beta1) beta cells, suggesting that beta cells may cycle through periods of high and low function, rather than existing in terminal states. We propose that a key branchpoint in the progression toward an immature state involves the attenuation of stress (HSF1downregulation), while other beta cells follow a trajectory toward UPR and cell proliferation involving XBP1 and MYC regulated gene programs.

Single-cell sequencing studies of beta cell heterogeneity in islets from individuals with obesity is limited by population size, BMI representation, and scope of analysis. Elevated BMI strongly associates with genes encoding electron transport chain complexes, ribosomal proteins, and insulin or related processing enzymes in human beta cells.[64,65] In contrast, many of these genes and pathways were downregulated in beta cells from donors with T2D,[11,64,65] suggesting their importance for beta cell compensation in obesity to maintain glucose homeostasis. *CD24* weakly correlated with BMI,[64] but was enriched in beta cells from T2D islets compared to healthy controls.[12] In obese *Lepr* KO mice, *Cd24* was enriched in immature beta cells (Beta3) although Beta3 cell abundance was lower compared to controls. These data may suggest a shift in *CD24* expression during chronic metabolic stress associates with islet decompensation resulting in dedifferentiation and loss of beta cell function in T2D.

In summary, our findings suggest MYC and XBP1 may coordinate transcriptional activities to upregulated cell cycle, ribosomal biogenesis, and translation gene programs to alleviate UPR and promote cell cycle progression leading to beta cell expansion in obesity. Our findings unify independently published observations on Myc[41,51,57] and UPR[9,42,53] regulated beta cell proliferation, while identifying aspects of stress attenuation and MYC transcriptional co-regulators central to obesity-induced beta cell proliferation. The presence of specific co-regulators, such as HCFC1 and WDR5, may determine specific gene programs activated by MYC during UPR and XBP1 activation to drive beta cell proliferation. Notably, these are the first scRNA-seq studies on obese female mice to our knowledge. Future studies will focus on the relationship of MYC and XBP1 to define the transcriptional complexes necessary for beta cell proliferation. Understanding the multifaceted pathways and beta cell subpopulations required for cell cycle progression will direct combinatorial targets to ensure full activation of beta cell proliferation, which may be a limitation of single target approaches. Thus, regenerative approaches for treating T1D may require coordinated targeting of MYC and XBP1 to restore functional beta cell mass and glucose control.

Limitations of the study

A limitation of this study is the need for orthogonal testing to validate the 6 beta cell subsets. While the subsets identified here are broadly consistent with published studies, it will be important to perform RNAscope as well as examine protein expression by immunostaining and cell sorting. Our single-cell data are a snapshot in time and we implemented commonly used tools to predict the relationship between clusters and the potential directionality of beta cell movement between them. It is possible there is bi-directional movement of beta cells between some clusters (i.e., Beta1 and Beta 3 or Beta1 and Beta2). Capturing single-cell transcriptomics at multiple timepoints would improve predictions of cell trajectory. For our study we selected female

mice, which are understudied, and while previous phenotyping of male and female *Lepr KO* mice was similar,[17] it will be important to determine if male mice exhibit similar transcriptional responses. Future studies are planned to use chemical and genetic tools to define the transcriptional mechanistic actions of MYC and XBP1 in obesity-induced beta cell proliferation.

RESOURCE AVAILABILITY

Lead contact

Further information and requests for resources and reagents should be directed to and will be fulfilled by the lead contact, Aaron Cox (Richard.A.Cox@uth.tmc.edu).

Materials availability

Ubc-Cre^{ERT2};Lepr$^{lp/lp}$ mice used in this study are available upon request. No other materials or reagents were generated by this study.

Data and code availability

The raw and processed scRNA-seq data reported in this paper are accessible through Gene Expression Omnibus (GSE262067). No original code was generated in this study. Any additional information required to reanalyze the data reported in this paper is available from the lead contact upon request.

ACKNOWLEDGMENTS

This work was funded by National Institutes of Health [R56DK128098, 1R03DK135458, and R01DK136694 to A.R.C., R01DK114356 and R01DK126042 to S.M.H.]. This study was also funded by Human Islets Research Network subaward (HIRN, RRID:SCR_014393; UC24 DK104162). This study was also funded (in part) by the BCM Bridge to Independence Program (A.R.C.). The Single Cell Genomics Core and RNA and Genomic Profiling Core are supported by NCI Cancer Center Support Grant P30CA125123. Graphical abstract was generated with Biorender.com.

AUTHOR CONTRIBUTIONS

Conceptualization, A.R.C. and S.M.H.; methodology, A.R.C., P.M.M., S.A.O., and N.J.M.; investigation, A.R.C., P.M.M., S.A.O., and N.J.M.; formal analysis, A.R.C., S.M.H., P.M.M., S.A.O., and N.J.M.; resources, A.R.C., S.M.H., and N.J.M.; writing – original draft, A.R.C., S.M.H., P.M.M., and N.J.M; writing – review and editing, A.R.C., S.M.H., and N.J.M.; funding acquisition, A.R.C. and S.M.H.; supervision, A.R.C., S.M.H., and N.J.M.

DECLARATION OF INTERESTS

The authors declare no competing interests.

STAR★METHODS

Detailed methods are provided in the online version of this paper and include the following:

- KEY RESOURCES TABLE
- EXPERIMENTAL MODEL AND STUDY PARTICIPANT DETAILS
  - Animal models
- METHOD DETAILS
  - Body weight and glucose homeostasis
  - Islet isolation
  - Single-cell RNA-sequencing
  - Analysis of scRNA-seq data
  - HCT target intersection analysis
- QUANTIFICATION AND STATISTICAL ANALYSIS

SUPPLEMENTAL INFORMATION

Supplemental information can be found online at https://doi.org/10.1016/j.isci.2025.112031.

Received: March 27, 2024
Revised: September 6, 2024
Accepted: February 11, 2025
Published: February 15, 2025

REFERENCES

1. Prentki, M., Peyot, M.-L., Masiello, P., and Madiraju, S.R.M. (2020). Nutrient-Induced Metabolic Stress, Adaptation, Detoxification, and Toxicity in the Pancreatic β-Cell. Diabetes *69*, 279–290. https://doi.org/10.2337/dbi19-0014.
2. Butler, A.E., Janson, J., Bonner-Weir, S., Ritzel, R., Rizza, R.A., and Butler, P.C. (2003). Beta-cell deficit and increased beta-cell apoptosis in humans with type 2 diabetes. Diabetes *52*, 102–110. https://doi.org/10.2337/diabetes.52.1.102.
3. Karaca, M., Castel, J., Tourrel-Cuzin, C., Brun, M., Géant, A., Dubois, M., Catesson, S., Rodriguez, M., Luquet, S., Cattan, P., et al. (2009). Exploring functional beta-cell heterogeneity in vivo using PSA-NCAM as a specific marker. PLoS One *4*, e5555. https://doi.org/10.1371/journal.pone.0005555.
4. Smukler, S.R., Arntfield, M.E., Razavi, R., Bikopoulos, G., Karpowicz, P., Seaberg, R., Dai, F., Lee, S., Ahrens, R., Fraser, P.E., et al. (2011). The adult mouse and human pancreas contain rare multipotent stem cells that express insulin. Cell Stem Cell *8*, 281–293. https://doi.org/10.1016/j.stem.2011.01.015.
5. Dorrell, C., Schug, J., Canaday, P.S., Russ, H.A., Tarlow, B.D., Grompe, M.T., Horton, T., Hebrok, M., Streeter, P.R., Kaestner, K.H., and Grompe, M. (2016). Human islets contain four distinct subtypes of β cells. Nat. Commun. *7*, 11756. https://doi.org/10.1038/ncomms11756.
6. Bader, E., Migliorini, A., Gegg, M., Moruzzi, N., Gerdes, J., Roscioni, S.S., Bakhti, M., Brandl, E., Irmler, M., Beckers, J., et al. (2016). Identification of proliferative and mature β-cells in the islets of Langerhans. Nature *535*, 430–434. https://doi.org/10.1038/nature18624.
7. Beamish, C.A., Strutt, B.J., Arany, E.J., and Hill, D.J. (2016). Insulin-positive, Glut2-low cells present within mouse pancreas exhibit lineage plasticity and are enriched within extra-islet endocrine cell clusters. Islets *8*, 65–82. https://doi.org/10.1080/19382014.2016.1162367.
8. van der Meulen, T., Mawla, A.M., DiGruccio, M.R., Adams, M.W., Nies, V., Dólleman, S., Liu, S., Ackermann, A.M., Cáceres, E., Hunter, A.E., et al. (2017). Virgin Beta Cells Persist throughout Life at a Neogenic Niche within Pancreatic Islets. Cell Metab. *25*, 911–926.e6. https://doi.org/10.1016/j.cmet.2017.03.017.
9. Xin, Y., Dominguez Gutierrez, G., Okamoto, H., Kim, J., Lee, A.-H., Adler, C., Ni, M., Yancopoulos, G.D., Murphy, A.J., and Gromada, J. (2018). Pseudotime Ordering of Single Human β-Cells Reveals States of Insulin Production and Unfolded Protein Response. Diabetes *67*, 1783–1794. https://doi.org/10.2337/db18-0365.
10. Zeng, C., Mulas, F., Sui, Y., Guan, T., Miller, N., Tan, Y., Liu, F., Jin, W., Carrano, A.C., Huising, M.O., et al. (2017). Pseudotemporal Ordering of Single Cells Reveals Metabolic Control of Postnatal β Cell Proliferation. Cell Metab. *25*, 1160–1175.e11. https://doi.org/10.1016/j.cmet.2017.04.014.
11. Camunas-Soler, J., Dai, X.-Q., Hang, Y., Bautista, A., Lyon, J., Suzuki, K., Kim, S.K., Quake, S.R., and MacDonald, P.E. (2020). Patch-Seq Links Single-Cell Transcriptomes to Human Islet Dysfunction in Diabetes. Cell Metab. *31*, 1017–1031.e4. https://doi.org/10.1016/j.cmet.2020.04.005.
12. Dror, E., Fagnocchi, L., Wegert, V., Apostle, S., Grimaldi, B., Gruber, T., Panzeri, I., Heyne, S., Höffler, K.D., Kreiner, V., et al. (2023). Epigenetic dosage identifies two major and functionally distinct β cell subtypes. Cell Metab. *35*, 821–836.e7. https://doi.org/10.1016/j.cmet.2023.03.008.

13. Rubio-Navarro, A., Gómez-Banoy, N., Stoll, L., Dündar, F., Mawla, A.M., Ma, L., Cortada, E., Zumbo, P., Li, A., Reiterer, M., et al. (2023). A beta cell subset with enhanced insulin secretion and glucose metabolism is reduced in type 2 diabetes. Nat. Cell Biol. *25*, 565–578. https://doi.org/10.1038/s41556-023-01103-1.

14. Kang, R.B., Li, Y., Rosselot, C., Zhang, T., Siddiq, M., Rajbhandari, P., Stewart, A.F., Scott, D.K., Garcia-Ocana, A., and Lu, G. (2023). Single-nucleus RNA sequencing of human pancreatic islets identifies novel gene sets and distinguishes β-cell subpopulations with dynamic transcriptome profiles. Genome Med. *15*, 30. https://doi.org/10.1186/s13073-023-01179-2.

15. Dor, Y., Brown, J., Martinez, O.I., and Melton, D.A. (2004). Adult pancreatic beta-cells are formed by self-duplication rather than stem-cell differentiation. Nature *429*, 41–46. https://doi.org/10.1038/nature02520.

16. Teta, M., Rankin, M.M., Long, S.Y., Stein, G.M., and Kushner, J.A. (2007). Growth and regeneration of adult beta cells does not involve specialized progenitors. Dev. Cell *12*, 817–826. https://doi.org/10.1016/j.devcel.2007.04.011.

17. Cox, A.R., Lam, C.J., Rankin, M.M., King, K.A., Chen, P., Martinez, R., Li, C., and Kushner, J.A. (2016). Extreme obesity induces massive beta cell expansion in mice through self-renewal and does not alter the beta cell lineage. Diabetologia *59*, 1231–1241. https://doi.org/10.1007/s00125-016-3922-7.

18. Bernal-Mizrachi, E., Kulkarni, R.N., Scott, D.K., Mauvais-Jarvis, F., Stewart, A.F., and Garcia-Ocaña, A. (2014). Human β-cell proliferation and intracellular signaling part 2: still driving in the dark without a road map. Diabetes *63*, 819–831. https://doi.org/10.2337/db13-1146.

19. Docherty, F.M., and Sussel, L. (2021). Islet Regeneration: Endogenous and Exogenous Approaches. Int. J. Mol. Sci. *22*, 3306. https://doi.org/10.3390/ijms22073306.

20. Teta, M., Long, S.Y., Wartschow, L.M., Rankin, M.M., and Kushner, J.A. (2005). Very slow turnover of beta-cells in aged adult mice. Diabetes *54*, 2557–2567. https://doi.org/10.2337/diabetes.54.9.2557.

21. Lam, C.J., Jacobson, D.R., Rankin, M.M., Cox, A.R., and Kushner, J.A. (2017). β Cells Persist in T1D Pancreata Without Evidence of Ongoing β-Cell Turnover or Neogenesis. J. Clin. Endocrinol. Metab. *102*, 2647–2659. https://doi.org/10.1210/jc.2016-3806.

22. Rankin, M.M., and Kushner, J.A. (2009). Adaptive beta-cell proliferation is severely restricted with advanced age. Diabetes *58*, 1365–1372. https://doi.org/10.2337/db08-1198.

23. Dai, C., Hang, Y., Shostak, A., Poffenberger, G., Hart, N., Prasad, N., Phillips, N., Levy, S.E., Greiner, D.L., Shultz, L.D., et al. (2017). Age-dependent human β cell proliferation induced by glucagon-like peptide 1 and calcineurin signaling. J. Clin. Investig. *127*, 3835–3844. https://doi.org/10.1172/JCI91761.

24. Rahier, J., Guiot, Y., Goebbels, R.M., Sempoux, C., and Henquin, J.C. (2008). Pancreatic beta-cell mass in European subjects with type 2 diabetes. Diabetes Obes. Metab. *10*, 32–42. https://doi.org/10.1111/j.1463-1326.2008.00969.x.

25. Bock, T., Pakkenberg, B., and Buschard, K. (2003). Increased islet volume but unchanged islet number in ob/ob mice. Diabetes *52*, 1716–1722. https://doi.org/10.2337/diabetes.52.7.1716.

26. Peyot, M.-L., Pepin, E., Lamontagne, J., Latour, M.G., Zarrouki, B., Lussier, R., Pineda, M., Jetton, T.L., Madiraju, S.R.M., Joly, E., and Prentki, M. (2010). Beta-cell failure in diet-induced obese mice stratified according to body weight gain: secretory dysfunction and altered islet lipid metabolism without steatosis or reduced beta-cell mass. Diabetes *59*, 2178–2187. https://doi.org/10.2337/db09-1452.

27. Stamateris, R.E., Sharma, R.B., Hollern, D.A., and Alonso, L.C. (2013). Adaptive β-cell proliferation increases early in high-fat feeding in mice, concurrent with metabolic changes, with induction of islet cyclin D2 expression. Am. J. Physiol. Endocrinol. Metab. *305*, E149–E159. https://doi.org/10.1152/ajpendo.00040.2013.

28. Chan, J.Y., Luzuriaga, J., Bensellam, M., Biden, T.J., and Laybutt, D.R. (2013). Failure of the adaptive unfolded protein response in islets of obese mice is linked with abnormalities in β-cell gene expression and progression to diabetes. Diabetes *62*, 1557–1568. https://doi.org/10.2337/db12-0701.

29. Dalbøge, L.S., Almholt, D.L.C., Neerup, T.S.R., Vassiliadis, E., Vrang, N., Pedersen, L., Fosgerau, K., and Jelsing, J. (2013). Characterisation of Age-Dependent Beta Cell Dynamics in the Male db/db Mice. PLoS One *8*, e82813. https://doi.org/10.1371/journal.pone.0082813.

30. Maachi, H., Ghislain, J., Tremblay, C., and Poitout, V. (2021). Pronounced proliferation of non-beta cells in response to beta-cell mitogens in isolated human islets of Langerhans. Sci. Rep. *11*, 11283. https://doi.org/10.1038/s41598-021-90643-3.

31. Maachi, H., Fergusson, G., Ethier, M., Brill, G.N., Katz, L.S., Honig, L.B., Metukuri, M.R., Scott, D.K., Ghislain, J., and Poitout, V. (2020). HB-EGF Signaling Is Required for Glucose-Induced Pancreatic β-Cell Proliferation in Rats. Diabetes *69*, 369–380. https://doi.org/10.2337/db19-0643.

32. Alonso, L.C., Yokoe, T., Zhang, P., Scott, D.K., Kim, S.K., O'Donnell, C.P., and Garcia-Ocaña, A. (2007). Glucose infusion in mice: a new model to induce beta-cell replication. Diabetes *56*, 1792–1801. https://doi.org/10.2337/db06-1513.

33. El Ouaamari, A., Dirice, E., Gedeon, N., Hu, J., Zhou, J.-Y., Shirakawa, J., Hou, L., Goodman, J., Karampelias, C., Qiang, G., et al. (2016). SerpinB1 Promotes Pancreatic β Cell Proliferation. Cell Metab. *23*, 194–205. https://doi.org/10.1016/j.cmet.2015.12.001.

34. Coate, K.C., Dai, C., Singh, A., Stanley, J., Covington, B.A., Bradley, A., Oladipupo, F., Gong, Y., Wisniewski, S., Sellick, K., et al. (2024). Interruption of glucagon signaling augments islet non-alpha cell proliferation in SLC7A2- and mTOR-dependent manners. Mol. Metab. *90*. https://doi.org/10.1016/j.molmet.2024.102050.

35. Moullé, V.S., Tremblay, C., Castell, A.-L., Vivot, K., Ethier, M., Fergusson, G., Alquier, T., Ghislain, J., and Poitout, V. (2019). The autonomic nervous system regulates pancreatic β-cell proliferation in adult male rats. Am. J. Physiol. Endocrinol. Metab. *317*, E234–E243. https://doi.org/10.1152/ajpendo.00385.2018.

36. Kondegowda, N.G., Fenutria, R., Pollack, I.R., Orthofer, M., Garcia-Ocaña, A., Penninger, J.M., and Vasavada, R.C. (2015). Osteoprotegerin and Denosumab Stimulate Human Beta Cell Proliferation through Inhibition of the Receptor Activator of NF-κB Ligand Pathway. Cell Metab. *22*, 77–85. https://doi.org/10.1016/j.cmet.2015.05.021.

37. Jalabert, A., Vial, G., Guay, C., Wiklander, O.P.B., Nordin, J.Z., Aswad, H., Forterre, A., Meugnier, E., Pesenti, S., Regazzi, R., et al. (2016). Exosome-like vesicles released from lipid-induced insulin-resistant muscles modulate gene expression and proliferation of beta recipient cells in mice. Diabetologia *59*, 1049–1058. https://doi.org/10.1007/s00125-016-3882-y.

38. Salinno, C., Büttner, M., Cota, P., Tritschler, S., Tarquis-Medina, M., Bastidas-Ponce, A., Scheibner, K., Burtscher, I., Böttcher, A., Theis, F.J., et al. (2021). CD81 marks immature and dedifferentiated pancreatic β-cells. Mol. Metab. *49*, 101188. https://doi.org/10.1016/j.molmet.2021.101188.

39. Piñeros, A.R., Gao, H., Wu, W., Liu, Y., Tersey, S.A., and Mirmira, R.G. (2020). Single-Cell Transcriptional Profiling of Mouse Islets Following Short-Term Obesogenic Dietary Intervention. Metabolites *10*, 513. https://doi.org/10.3390/metabo10120513.

40. Tatsuoka, H., Sakamoto, S., Yabe, D., Kabai, R., Kato, U., Okumura, T., Botagarova, A., Tokumoto, S., Usui, R., Ogura, M., et al. (2020). Single-Cell Transcriptome Analysis Dissects the Replicating Process of Pancreatic Beta Cells in Partial Pancreatectomy Model. iScience *23*, 101774. https://doi.org/10.1016/j.isci.2020.101774.

41. Vivoli, A., Ghislain, J., Filali-Mouhim, A., Angeles, Z.E., Castell, A.-L., Sladek, R., and Poitout, V. (2023). Single-Cell RNA Sequencing Reveals a Role for Reactive Oxygen Species and Peroxiredoxins in Fatty

Acid-Induced Rat β-Cell Proliferation. Diabetes *72*, 45–58. https://doi.org/10.2337/db22-0121.

42. Sharma, R.B., O'Donnell, A.C., Stamateris, R.E., Ha, B., McCloskey, K.M., Reynolds, P.R., Arvan, P., and Alonso, L.C. (2015). Insulin demand regulates β cell number via the unfolded protein response. J. Clin. Investig. *125*, 3831–3846. https://doi.org/10.1172/JCI79264.
43. Shi, Y., Mosser, D.D., and Morimoto, R.I. (1998). Molecular chaperones as HSF1-specific transcriptional repressors. Gen. Dev. *12*, 654–666. https://doi.org/10.1101/gad.12.5.654.
44. Ochsner, S.A., Abraham, D., Martin, K., Ding, W., McOwiti, A., Kankanamge, W., Wang, Z., Andreano, K., Hamilton, R.A., Chen, Y., et al. (2019). The Signaling Pathways Project, an integrated 'omics knowledgebase for mammalian cellular signaling pathways. Sci. Data *6*, 252. https://doi.org/10.1038/s41597-019-0193-4.
45. Ochsner, S.A., Pillich, R.T., and McKenna, N.J. (2020). Consensus transcriptional regulatory networks of coronavirus-infected human cells. Sci. Data *7*, 314. https://doi.org/10.1038/s41597-020-00628-6.
46. Ochsner, S.A., Pillich, R.T., Rawool, D., Grethe, J.S., and McKenna, N.J. (2022). Transcriptional regulatory networks of circulating immune cells in type 1 diabetes: A community knowledgebase. iScience *25*, 104581. https://doi.org/10.1016/j.isci.2022.104581.
47. Bissig-Choisat, B., Alves-Bezerra, M., Zorman, B., Ochsner, S.A., Barzi, M., Legras, X., Yang, D., Borowiak, M., Dean, A.M., York, R.B., et al. (2021). A human liver chimeric mouse model for non-alcoholic fatty liver disease. JHEP Rep. *3*, 100281. https://doi.org/10.1016/j.jhepr.2021.100281.
48. Michaud, J., Praz, V., James Faresse, N., Jnbaptiste, C.K., Tyagi, S., Schütz, F., and Herr, W. (2013). HCFC1 is a common component of active human CpG-island promoters and coincides with ZNF143, THAP11, YY1, and GABP transcription factor occupancy. Gen. Res. *23*, 907–916. https://doi.org/10.1101/gr.150078.112.
49. Parker, J.B., Yin, H., Vinckevicius, A., and Chakravarti, D. (2014). Host cell factor-1 recruitment to E2F-bound and cell-cycle-control genes is mediated by THAP11 and ZNF143. Cell Rep. *9*, 967–982. https://doi.org/10.1016/j.celrep.2014.09.051.
50. Chung, J.-Y., Ma, Y., Zhang, D., Bickerton, H.H., Stokes, E., Patel, S.B., Tse, H.M., Feduska, J., Welner, R.S., and Banerjee, R.R. (2023). Pancreatic islet cell type–specific transcriptomic changes during pregnancy and postpartum. iScience *26*, 106439. https://doi.org/10.1016/j.isci.2023.106439.
51. Rosselot, C., Kumar, A., Lakshmipathi, J., Zhang, P., Lu, G., Katz, L.S., Prochownik, E.V., Stewart, A.F., Lambertini, L., Scott, D.K., and Garcia-Ocaña, A. (2019). Myc Is Required for Adaptive β-Cell Replication in Young Mice but Is Not Sufficient in One-Year-Old Mice Fed With a High-Fat Diet. Diabetes *68*, 1934–1949. https://doi.org/10.2337/db18-1368.
52. Eizirik, D.L., Cardozo, A.K., and Cnop, M. (2008). The role for endoplasmic reticulum stress in diabetes mellitus. Endocr. Rev. *29*, 42–61. https://doi.org/10.1210/er.2007-0015.
53. Szabat, M., Page, M.M., Panzhinskiy, E., Skovsø, S., Mojibian, M., Fernandez-Tajes, J., Bruin, J.E., Bround, M.J., Lee, J.T.C., Xu, E.E., et al. (2016). Reduced Insulin Production Relieves Endoplasmic Reticulum Stress and Induces β Cell Proliferation. Cell Metab. *23*, 179–193. https://doi.org/10.1016/j.cmet.2015.10.016.
54. Charbord, J., Ren, L., Sharma, R.B., Johansson, A., Ågren, R., Chu, L., Tworus, D., Schulz, N., Charbord, P., Stewart, A.F., et al. (2021). In vivo screen identifies a SIK inhibitor that induces β cell proliferation through a transient UPR. Nat. Metab. *3*, 682–700. https://doi.org/10.1038/s42255-021-00391-x.
55. Zhao, N., Cao, J., Xu, L., Tang, Q., Dobrolecki, L.E., Lv, X., Talukdar, M., Lu, Y., Wang, X., Hu, D.Z., et al. (2018). Pharmacological targeting of MYC-regulated IRE1/XBP1 pathway suppresses MYC-driven breast cancer. J. Clin. Investig. *128*, 1283–1299. https://doi.org/10.1172/JCI95873.
56. Sheng, X., Nenseth, H.Z., Qu, S., Kuzu, O.F., Frahnow, T., Simon, L., Greene, S., Zeng, Q., Fazli, L., Rennie, P.S., et al. (2019). IRE1α-XBP1s pathway promotes prostate cancer by activating c-MYC signaling. Nat. Commun. *10*, 323. https://doi.org/10.1038/s41467-018-08152-3.
57. Karslioglu, E., Kleinberger, J.W., Salim, F.G., Cox, A.E., Takane, K.K., Scott, D.K., and Stewart, A.F. (2011). cMyc is a principal upstream driver of beta-cell proliferation in rat insulinoma cell lines and is an effective mediator of human beta-cell replication. Mol. Endocrinol. *25*, 1760–1772. https://doi.org/10.1210/me.2011-1074.
58. Dai, M.-S., and Lu, H. (2008). Crosstalk between c-Myc and ribosome in ribosomal biogenesis and cancer. J. Cell. Biochem. *105*, 670–677. https://doi.org/10.1002/jcb.21895.
59. Moss, T. (2004). At the crossroads of growth control; making ribosomal RNA. Curr. Opin. Genet. Dev. *14*, 210–217. https://doi.org/10.1016/j.gde.2004.02.005.
60. Thomas, L.R., Wang, Q., Grieb, B.C., Phan, J., Foshage, A.M., Sun, Q., Olejniczak, E.T., Clark, T., Dey, S., Lorey, S., et al. (2015). Interaction with WDR5 promotes target gene recognition and tumorigenesis by MYC. Mol. Cell *58*, 440–452. https://doi.org/10.1016/j.molcel.2015.02.028.
61. Thomas, L.R., Adams, C.M., Wang, J., Weissmiller, A.M., Creighton, J., Lorey, S.L., Liu, Q., Fesik, S.W., Eischen, C.M., and Tansey, W.P. (2019). Interaction of the oncoprotein transcription factor MYC with its chromatin cofactor WDR5 is essential for tumor maintenance. Proc. Natl. Acad. Sci. USA *116*, 25260–25268. https://doi.org/10.1073/pnas.1910391116.
62. Popay, T.M., Wang, J., Adams, C.M., Howard, G.C., Codreanu, S.G., Sherrod, S.D., McLean, J.A., Thomas, L.R., Lorey, S.L., Machida, Y.J., et al. (2021). MYC regulates ribosome biogenesis and mitochondrial gene expression programs through its interaction with host cell factor-1. Elife *10*, e60191. https://doi.org/10.7554/eLife.60191.
63. Xiang, P., Li, F., Ma, Z., Yue, J., Lu, C., You, Y., Hou, L., Yin, B., Qiang, B., Shu, P., and Peng, X. (2020). HCF-1 promotes cell cycle progression by regulating the expression of CDC42. Cell Death Dis. *11*, 907. https://doi.org/10.1038/s41419-020-03094-5.
64. Segerstolpe, Å., Palasantza, A., Eliasson, P., Andersson, E.-M., Andréasson, A.-C., Sun, X., Picelli, S., Sabirsh, A., Clausen, M., Bjursell, M.K., et al. (2016). Single-Cell Transcriptome Profiling of Human Pancreatic Islets in Health and Type 2 Diabetes. Cell Metab. *24*, 593–607. https://doi.org/10.1016/j.cmet.2016.08.020.
65. Fang, Z., Weng, C., Li, H., Tao, R., Mai, W., Liu, X., Lu, L., Lai, S., Duan, Q., Alvarez, C., et al. (2019). Single-Cell Heterogeneity Analysis and CRISPR Screen Identify Key β-Cell-Specific Disease Genes. Cell Rep. *26*, 3132–3144.e7. https://doi.org/10.1016/j.celrep.2019.02.043.
66. Hao, Y., Hao, S., Andersen-Nissen, E., Mauck, W.M., Zheng, S., Butler, A., Lee, M.J., Wilk, A.J., Darby, C., Zager, M., et al. (2021). Integrated analysis of multimodal single-cell data. Cell *184*, 3573–3587.e29. https://doi.org/10.1016/j.cell.2021.04.048.
67. Nestorowa, S., Hamey, F.K., Pijuan Sala, B., Diamanti, E., Shepherd, M., Laurenti, E., Wilson, N.K., Kent, D.G., and Göttgens, B. (2016). A single-cell resolution map of mouse hematopoietic stem and progenitor cell differentiation. Blood *128*, e20–e31. https://doi.org/10.1182/blood-2016-05-716480.
68. Subramanian, A., Tamayo, P., Mootha, V.K., Mukherjee, S., Ebert, B.L., Gillette, M.A., Paulovich, A., Pomeroy, S.L., Golub, T.R., Lander, E.S., and Mesirov, J.P. (2005). Gene set enrichment analysis: a knowledge-based approach for interpreting genome-wide expression profiles. Proc. Natl. Acad. Sci. USA *102*, 15545–15550. https://doi.org/10.1073/pnas.0506580102.
69. Liberzon, A., Birger, C., Thorvaldsdóttir, H., Ghandi, M., Mesirov, J.P., and Tamayo, P. (2015). The Molecular Signatures Database (MSigDB) hallmark gene set collection. Cell Syst. *1*, 417–425. https://doi.org/10.1016/j.cels.2015.12.004.
70. Fabregat, A., Sidiropoulos, K., Viteri, G., Forner, O., Marin-Garcia, P., Arnau, V., D'Eustachio, P., Stein, L., and Hermjakob, H. (2017). Reactome pathway analysis: a high-performance in-memory approach. BMC Bioinf. *18*, 142. https://doi.org/10.1186/s12859-017-1559-2.

71. Trapnell, C., Cacchiarelli, D., Grimsby, J., Pokharel, P., Li, S., Morse, M., Lennon, N.J., Livak, K.J., Mikkelsen, T.S., and Rinn, J.L. (2014). The dynamics and regulators of cell fate decisions are revealed by pseudotemporal ordering of single cells. Nat. Biotechnol. *32*, 381–386. https://doi.org/10.1038/nbt.2859.

72. Cao, J., Spielmann, M., Qiu, X., Huang, X., Ibrahim, D.M., Hill, A.J., Zhang, F., Mundlos, S., Christiansen, L., Steemers, F.J., et al. (2019). The single-cell transcriptional landscape of mammalian organogenesis. Nature *566*, 496–502. https://doi.org/10.1038/s41586-019-0969-x.

73. Oki, S., Ohta, T., Shioi, G., Hatanaka, H., Ogasawara, O., Okuda, Y., Kawaji, H., Nakaki, R., Sese, J., and Meno, C. (2018). ChIP-Atlas: a data-mining suite powered by full integration of public ChIP-seq data. EMBO Rep. *19*, e46255. https://doi.org/10.15252/embr.201846255.

STAR★METHODS

KEY RESOURCES TABLE

REAGENT or RESOURCE	SOURCE	IDENTIFIER
Chemicals, peptides, and recombinant proteins		
Collagenase type V	Sigma Aldrich	Cat#9263
Hank's Balanced Salt Solution	Thermo Fisher	Cat#14025092
RPMI 1640	Thermo Fisher	Cat#11875093
Tamoxifen	MP Biomedicals	Cat#215673891
TrypLE Express	Thermo Fisher	Cat#12604013
Critical commercial assays		
Single-cell 3′ reagent kit v3.1	10× Genomics	Cat#PN-1000268
Deposited data		
scRNA-seq data	GEO	GSE262067
Experimental models: Organisms/strains		
Mouse: Ubc-CreERT2; Lepr-lp/lp	Cox et al.[17]	N/A
Oligonucleotides		
See Table S10	Integrated DNA Technologies	N/A
Software and algorithms		
GraphPad Prism 10	Dotmatics	N/A
Cell Ranger v3.1	10× Genomics	N/A
R	https://www.r-project.org	RRID:SCR_001905
RStudio 4.0.0	https://www.rstudio.com	RRID:SCR_000432
Seurat	Hao et al.[63]	RRID:SCR_007322
Gene Set Enrichment Analysis	Subramanian et al.[65]; Liberzon et al.[66]	RRID:SCR_003199
Reactome	Fabregat et al.[67]	RRID:SCR_003485
Monocle 3	Trapnell et al.[68]; Cao et al.[69]	RRID:SCR_018685

EXPERIMENTAL MODEL AND STUDY PARTICIPANT DETAILS

Animal models

All mice (*mus musculus*) were housed in a pathogen-free animal facility with 12 h dark-light cycle and free access to water and food. *Ubc-Cre^{ERT2};Lepr$^{lp/lp}$* and littermate *Lepr$^{lp/lp}$* mice were generated previously,[17] with both female and male mice exhibiting similar phenotypes. Female mice at 3-months of age were used in the current studies. All animal procedures complied with and were approved (AN-8873) by the Institutional Animal Care and Use Committee of Baylor College of Medicine. All experiments adhered to ARRIVE Guidelines.

METHOD DETAILS

Body weight and glucose homeostasis

Three-month-old female *Ubc-Cre^{ERT2};Lepr$^{lp/lp}$* and littermate control (*Lepr$^{lp/lp}$*) mice were treated with 0.1 mg/g tamoxifen body weight by oral gavage for 5 consecutive days, beginning on day 0[17]. Tamoxifen dose was selected with the lowest toxicity to beta cells that would still induce sufficient recombination and obesity. Body weight was recorded during the study and final random fed blood glucose measured. An insulin tolerance test (1 U/kg body weight) was performed 1 day before sacrifice. At day 9, during a period of elevated beta cell proliferation,[17] mice were anesthetized with isoflurane for islet isolation. Mice were euthanized by cervical dislocation and bilateral thoracotomy.

Islet isolation

The pancreas was perfused through the bile duct with 1–2 mL of collagenase type V (2 mg/mL; Sigma Aldrich #9263) in HBSS (Thermo Fisher #14025092). The pancreas was removed and placed in a 50 mL conical with 3–5 mL of collagenase (2 mg/mL) in HBSS. Samples were placed in a shaking incubator at 37°C for 5–6 min. Digestion was stopped by adding 45 mL of cold RPMI

(Thermo Fisher #11875093) + 10% FBS. Samples were centrifuged at 339xg at 4°C for 2 min using swing buckets. Supernatant was removed, the pellet was resuspended in 10 mL of cold RPMI +10% FBS and transferred to a 10 cm non-tissue culture dish. Islets were hand picked into 1.5 mL tubes. To ensure a clean and pure islet prep, islets were handpicked 2 more times and then transferred to 5 mL polystyrene tubes for generation of single cell suspension. Two mL RPMI +10% FBS was added and then centrifuged at 339xg at 4°C for 2 min using swing buckets. Supernatant was removed and pellets were resuspended in 1 mL of pre-warmed TrypLE Express (Thermo Fisher #12604013) and incubated for 10 min at 37°C with pipetting up and down every 2 min to facilitate dispersion. To stop, 2 mL of cold RPMI +10% FBS was added and the suspension was strained through a 40 μm filter. Supernatant was removed and pellets resuspend in 250 μL of cold RPMI +10% FBS for viability and cell counting.

Single-cell RNA-sequencing

Islets were pooled from 4 mice/group for each of *Lepr* KO and littermate controls for generating single cell suspensions. Single-cell capture and cDNA libraries were prepared by the Baylor College of Medicine Single Cell Genomics Core according to manufacturer's protocols (10× Genomics). Single-cell suspensions (~1000 cells/μl in PBS) were loaded into a microfluidic chip and placed in the 10× Genomics Chromium Controller to generate single-cell gel beads in emulsion with a targeted cell recovery of 10,000 cells. cDNA libraries were prepared with chromium single-cell 3′ reagent kit v3.1 (10× Genomics). The Baylor College of Medicine Genomic and RNA Profiling Core performed quality control with Bioanalyzer High Sensitivity DNA Analysis (Agilent) and sequencing on Illumina NovaSeq 6000 using PE150 to generate ~300M reads/sample.

Analysis of scRNA-seq data

Cell Ranger software v3.1 (10× Genomics) with default settings was used for alignment, barcode assignment, and UMI counting of the raw sequencing data with UCSC mouse genome reference mm9. Expression data was analyzed with Seurat 4.0 (https://satijalab.org/seurat)[66] using R Studio. Cells with detected genes <600, total features >6500, or mitochondrial DNA percent >10% were removed. Control and *Lepr* KO datasets were merged and integrated using the functions FindIntegrationAnchors and IntegrateData. The integrated data were scaled, and principal component analysis (PCA) was performed. Cell clusters were identified using FindClusters (16 principal components, resolution = 0.5). Cluster markers were defined by min.pct $\geq$0.25 and logfc.threshold $\geq$0.25, with ranking by average $\log_2$(fold change). The cell clusters were visualized using Uniform Manifold Approximation and Projection (UMAP) plots. Cell clusters were manually assigned based on known marker genes. The $\log_2$(fold change) data were plotted using the vinplot and doheatmap functions in Seurat. Differentially expressed genes (DEG) between control and *Lepr* KO were determined by DEseq. Cell cycle analysis was performed using the CellCycleScoring function.[67] Gene set enrichment analysis (GSEA) was performed using the Molecular Signatures Database[68,69] and reactome.org.[70] Trajectory and pseudotime analyses were performed using Monocle3.[71,72]

HCT target intersection analysis

High confidence transcript (HCT) intersection analysis[45] was used to compute the overlap between *Lepr* KO differentially expressed genes and ChIP-Seq consensome sets of 690 mouse signaling pathway nodes. Briefly from Ochsner et al.,[46] ChIP-Seq consensomes rank genes based on average peak height of a gene compared to all public ChIP-Seq datasets (ChIP-Atlas resource[73]) in which a specific node was an IP antigen.[44] Genes in the top 5% of these consensomes were designated as high confidence transcriptional targets (HCTs) for a given node.[45] We input the *Lepr* KO differentially expressed gene lists into the Bioconductor GeneOverlap analysis package in R to calculate the significant overlap with node HCTs. The enrichment (ENR) number represents the ratio of the number of observed intersecting genes and the number of expected intersecting genes. The problem was formulated as a hypergeometric distribution or contingency table and solved by Fisher's exact test. *p* values were adjusted for multiple testing by using the method of Benjamini & Hochberg to control the false discovery rate as implemented with the p.adjust function in R, to generate q values. The universe for the intersection was set at a conservative estimate of the total number of transcribed (protein and non-protein-coding) genes in the mouse genome (25,000).

QUANTIFICATION AND STATISTICAL ANALYSIS

Statistical analysis of metabolic parameters and qPCR was performed with GraphPad Prism v10. A two-way ANOVA was used to compare two variables (time vs. metabolic parameter) across two groups with a mixed-effects analysis. A Mann-Whitney U test (unpaired t-test) was used for fed glucose and qPCR gene expression data comparing two groups. Statistical analysis for scRNA-seq and HCT node enrichment are described in the respective method sections. Statistical analysis of GSEA datasets used hypergeometric testing of overrepresentation. A *p*-value <0.05 was considered significant, unless otherwise stated in the Figure Legends. All summary statistics are presented as mean ± SEM, with samples sizes indicated in each Figure Legend.